PROCEEDINGS OF SPIE

SPIEDigitalLibrary.org/conference-proceedings-of-spie

Structural and optical properties of indium-doped highly-conductive ZnO bulk crystals grown by the hydrothermal technique

Buguo Wang, Bruce Claflin, David Look, Juan Jiménez

Buguo Wang, Bruce Claflin, David Look, Juan Jiménez , "Structural and optical properties of indium-doped highly-conductive ZnO bulk crystals grown by the hydrothermal technique," Proc. SPIE 10533, Oxide-based Materials and Devices IX, 105331H (23 February 2018); doi: 10.1117/12.2289992

SPIE.

Event: SPIE OPTO, 2018, San Francisco, California, United States

Structural and optical properties of indium-doped highly-conductive ZnO bulk crystals grown by the hydrothermal technique

Buguo Wang [1*], Bruce Claflin [2], David Look [1,2], Juan Jiménez [3]

[1] *Semiconductor Research Center, Wright State University, Dayton, OH 45435, USA*
[2] *Sensors Directorate, Air Force Research Laboratory, Wright-Patterson AFB, OH 45433, USA*
[3] *Universidad de Valladolid, 47011-Valladolid, Spain*

ABSTRACT

Indium-doped ZnO bulk crystals grown by the hydrothermal method are highly-conductive, with resistivity at 0.01 Ωcm at room temperature as revealed by Hall-effect measurement. In this paper we report on structural and optical properties of these crystals. The grown In:ZnO crystals have been studied by high resolution X-ray diffraction, micro-Raman scattering and low-temperature photoluminescence and cathodoluminescence. It was found that the *c* lattice parameter of the grown In:ZnO crystal expanded 0.06% with respect to the lithium-doped ZnO crystal seed, and the In-doped ZnO overgrew the seed crystal pseudomorphically but with high quality crystallinity; the X-ray rocking curves show the FWHM of the Zn face and O faces are only 0.05^o and 0.1^o; and the indium concentration in the crystal reaches the solubility limit. Raman spectra show strain relaxation gradually from the regrowth interface as well as a weak spectral feature at 723 cm^{-1}. The peak at 312 cm^{-1} noticed in hydrothermally grown In:ZnO nanostructures does not appear in our In-doped crystals, indicating that this peak may be associated with specific defects (e.g. surface related) of the nanostructures. Photoluminescence measurements show that an indium donor bound exciton peak I_9 (In^0X) is the dominant peak in the PL spectrum, located at 3.3586 eV on the zinc face and 3.3577 eV on the oxygen face. Both of them deviated from the consensus literature value of 3.3567 eV, probably due to strain in the crystal induced by impurities.

Keywords: A1. ZnO conducting substrate, A1. Indium-doped ZnO, A1. X-ray diffraction, A2. hydrothermal growth, B3. Photoluminescence, B3. Micro-Raman

* E-mail: buguo.wang@wright.edu, phone: 937-775-3525

1. INTRODUCTION

Transparent conducting oxides (TCOs) have found many applications in several optoelectronic devices such as light emitting diodes (LEDs), solar cells, and displays, among other. As TCOs, ZnO-based materials, especially indium, gallium and aluminum (Group III)-doped ZnO crystals have demonstrated some advantages over other materials [1-2]. In addition, group-III doped ZnO also has many other applications, for example, as alpha-particle fast scintillators and as plasmonic materials [3].

Group III-doped ZnO films have been prepared by various techniques such as pulsed laser deposition (PLD) and liquid phase epitaxy (LPE) [4-5]. There are many reports on the photoluminescence, Raman

Oxide-based Materials and Devices IX, edited by David J. Rogers, David C. Look, Ferechteh H. Teherani, Proc. of SPIE Vol. 10533, 105331H · © 2018 SPIE
CCC code: 0277-786X/18/$18 · doi: 10.1117/12.2289992

spectroscopy, and electrical properties of group III doped ZnO thin films grown by these techniques in the literature, and also extensive research on the impurity defects [6-8]. However, there are only a few reports on the bulk growth and properties of group-III doped ZnO crystals.

Efficient long lifetime ZnO-based LEDs and laser diodes need low defect density homogeneous substrates. Hydrothermal growth offers a low-cost method for producing large area ZnO substrates, generally, with low electrical conductivity, however, optoelectronic devices require conducting ZnO substrates. Therefore a methodology is needed to produce low-cost, large-area conducting ZnO substrates. We have recently performed a series of crystal growth experiments to intentionally dope ZnO crystals with Ga, Al, and In by the hydrothermal method [9-11]. The experimental results showed that highly-conductive ZnO bulk substrates doped with group III ions can be grown by the hydrothermal technique. In particular, the In-doped ZnO crystals have a resistivity as low as 0.01 Ωcm at room temperature, among the lowest values measured for bulk conducting oxide materials. We report herein the special ZnO growth characteristics in the presence of indium ions in the hydrothermal solution, and we investigate the properties of the bulk In-doped ZnO crystals grown by the hydrothermal method, using high-resolution X-ray diffraction, micro-Raman spectroscopy, photoluminescence (PL) and cathodoluminescence (CL) [9-10].

2. EXPERIMENTAL

2.1 Indium-doped ZnO crystal growth

Indium-doped conducting ZnO crystals were grown by the hydrothermal technique. The (0001) plates of lithium-doped (nominally-undoped) ZnO cut from previous hydrothermal growth runs were used as seeds. A 4N KOH was used as the growth solution, which contained 0.01-0.04 M In_2O_3 (0.22%-0.55% molar ratio of In_2O_3 in the ZnO nutrient) for doping. Detailed growth conditions are similar to regular ZnO hydrothermal growth and can be found in our previous publications [9-11].

2.2 Characterization

The In-doped ZnO crystal was characterized by high-resolution x-ray diffraction (HRXRD) using monochromatic CuKα_1 radiation (λ = 1.540598 Å). A reciprocal space map (RSM) was measured for the (0004), (10-14), and (1-104) planes without dismounting the crystal.

An uncut, unpolished crystal was mounted on a PANalytical X'Pert MRD Eularian wafer cradle with the c+ or c- plane exposed. The incident beam optics included a Ge (220) symmetric 4-bounce monochromator (line source) and a parabolic mirror in extended mode. A beam spot of approximately 1mm × 1mm was used and the beam was centered on the c face. The detector optics was a triple-axis detector with 18" acceptance. The detector angle (2θ) was set to zero using the straight through (open) beam. The sample was iteratively aligned in the ω-, 2θ-, and χ-axes to optimize signal intensity and peak symmetry. As a control, a similarly grown sample of undoped ZnO was measured first.

Room-temperature (RT) and low-temperature (LT) photoluminescence (PL) were performed on as-grown samples. The RT PL was measured with a 0.25 *m* grating monochrometer, a CCD detector, and a 275 nm, 5 ns pulsed laser source, while the LT PL was measured with a 1.26 m grating spectrometer, a 325 nm CW He-Cd laser, and an RCA C31034A photomultiplier.

The CL measurements were carried out with a MonoCL2 system from Gatan UK, attached to a field-emission scanning electron microscope (FESEM-LEO 1530) [12]. Panchromatic CL images were acquired with a

photomultiplier tube, while the CL spectra were acquired with a Peltier-cooled CCD. The measurements were carried out at 80 K. The acceleration voltage of the e-beam was 20 kV, which the probe depth is ≈ 900 nm, neglecting thus the surface effects.

Micro-Raman spectroscopy measurements were performed on c planes the In:ZnO sample using a Renishaw confocal microscope system operated in backscattering geometry. The 514 nm line of an Ar+ laser was used as the excitation source and a 100× objective lens was used to focus the laser to ~1 μm diameter spot and to collect the scattered light.

3. RESULTS AND DISCUSSION

3.1 Surface morphology and crystal quality

Indium ions in the hydrothermal solution have a considerable influence on ZnO crystal morphology [9]. ZnO crystals grown in conventional hydrothermal solvents typically have (0001), (000-1), (10-11), (10-1-1) and (10-10) growth faces. The (0001) face has the fastest growth rate, followed by the (10-11), (10-10), (10-1-1) and (000-1) faces. Li^+ is usually added to hydrothermal solvents to improve ZnO crystal quality, and has no significant influence on the crystal morphology. However, with the addition of indium ions to the solution the crystals exhibit a plate-like morphology, as shown in Fig.1 (a). In other words, {0001} faces of ZnO have a little growth. We have used this growth characteristic to increase the diameter of c-plate ZnO seeds along the *m* planes, and up to 2" In-doped ZnO bulk crystals have been successfully grown by the hydrothermal technique in our laboratory. We have investigated the influence of impurity ions, particularly In^{3+}, on the ZnO hydrothermal growth mechanism, as finding that indium ions block the growth of {0001} faces. The (0001) surface has a number of growth hillocks arising from the indium contamination. Otherwise, the surface of new growth area is smooth and of high quality despite there are growth zones overlapped on the {0001} faces, observed on the cross-section (11-20), as shown in Fig.1 (b). The full width at half maximum (FWHM) of X-ray diffraction rocking curves measured on the (0001) and (000-1) of the crystal are 0.05^o and 0.1^o respectively, as shown in Fig.2, indicating high crystal quality. The FWHMs are slightly larger than those measured on nominally-undoped high quality ZnO crystals, which usually have a FWHM around 0.01^o or below.

The *a*- and *c*-parameters of pure hexagonal ZnO are 3.2498 Å and 5.2066 Å, respectively. X-ray diffraction on the doped crystal showed that the *a*-parameter is 3.243Å, which is 0.2% lower than the pure ZnO value [13], and the *c*-parameter is 5.210 Å, greater than the undoped lattice constant. The relative change in the *c*-parameter between the seed and the overgrowth is 0.06%. Indium has a larger ionic radius than zinc [14]. In_2O_3 has an Ia3 space group with lattice constant a=10.117Å which is bigger than *c* constant of wurtzite ZnO [15]. Doped indium substitutes zinc and forms an octahedral coordination with oxygen. However, zinc has tetrahedral coordination with oxygen. In order to keep the ZnO structure unchanged, it is assumed that the diagonal of the indium coordinated octahedra tends to be parallel to the c axis of the ZnO lattice. More longitudinal space is needed to accommodate the substituent indium in the ZnO lattices. Therefore, the doped crystal has an expanded *c* constant while the *a* lattice constant shows little change. The Li-doped ZnO seed should have a smaller lattice constant; however, indium can diffuse into the ZnO seed resulting in a larger lattice constant of the seed, than that of a "true" lithium-doped ZnO. We observed that, even without any doping growth, the ZnO seeds can be contaminated with indium by diffusion in the hydrothermal solutions containing In^{3+}.

In short, Li from the mineralizer LiOH is known to incorporate into Zn sites to shrink the lattice [16], while In incorporates into ZnO to expand the lattice [17]. The overgrowth completely encases the seed crystal. Elastic-strain sharing would affect both the seed and overgrowth lattice parameters. Because each face grows at different

rates, we can expect a stress imbalance to bend the crystal. On the other hand, since the hydrothermal growth is a growth at near-equilibrium, the dopant concentration in the crystal is determined by the solubility. It was found that the indium concentration in the hydrothermal In:ZnO crystal can reach the solubility limit of 1×10^{19} cm^{-3} for In^{3+} in ZnO, similar to gallium and aluminum doped hydrothermal ZnO growth at the near-equilibrium growth, as shown in Table 1.

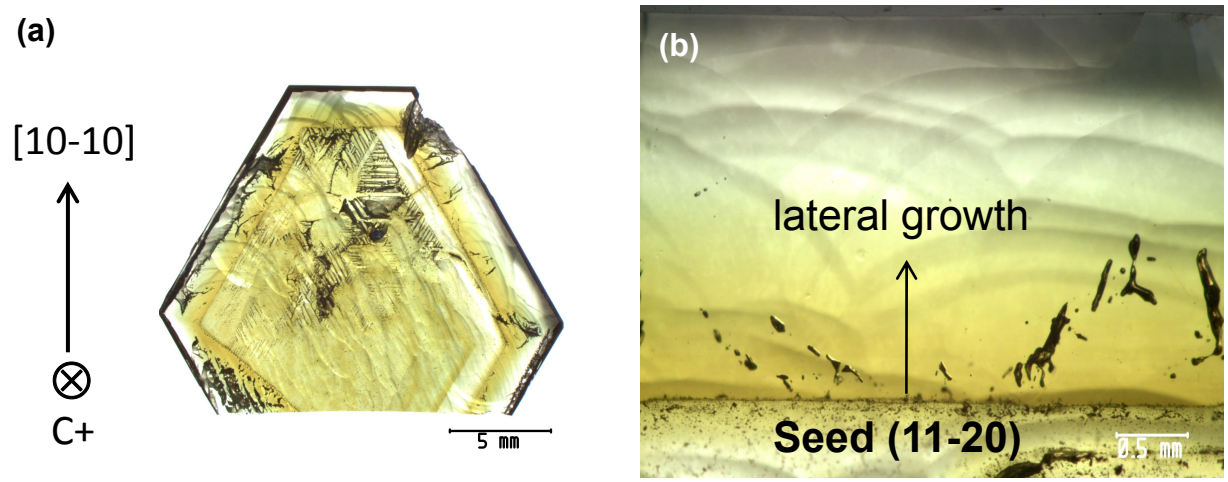

Fig.1. (a) Photograph of an as-grown In-doped ZnO crystal grown by the hydrothermal method. The seed can be clearly seen inside along with the new growth on the edges. The crystal is about 650 μm thick, with new growth of 150 μm on the O face and 250 μm on the Zn face. (b) Micromorphology of a polished (11-20) cross-section of an In:ZnO crystal, showing a high quality doping growth on a lithium-doped seed.

Table 1. The doping concentrations measured in group III-doped hydrothermal ZnO crystals and the solubility of group III in ZnO reported in literature

	Indium	Gallium	Aluminum
This work	1.6×10^{19}	7.2×10^{18}	3.1×10^{19}
Literature [21-22]	1×10^{19}	1×10^{19}	1×10^{19}

Observation of the {0001} surfaces of the In:ZnO crystal under microscopy reveals the presence of six-fold symmetrical hillocks. These hillocks were studied by CL. The panchromatic image of one of those hillocks is shown in Fig.3a. Monochromatic CL images of the near band edge (NBE) emission and the deep level emission (orange band) are shown in Fig. 3b and 3c respectively. The bright emission of the hillock is due to the orange emission, while the NBE emission is the dominant one out of the hillock. Local CL spectra acquired in the points indicated in Fig.3b are shown in Fig. 3d. The CL spectra recorded inside the hillock show a strong orange luminescence emission peaking at around 2.05 eV, while the NBE emission is not observed. Only the core of the hillock exhibits

the NBE emission, with a dominant peak at 3.304 eV and some weak phonon replicas. The spectrum out of the hillock shows a peak at 3.34 eV, which can be related to the I_9 peak usually associated with an exciton bound to In donors, the deep level luminescence is almost nonexistent in this region. The overall luminescence is more intense in the hillock, which suggests a higher concentration of non-radiative recombination centers in the smooth region out of the hillocks.

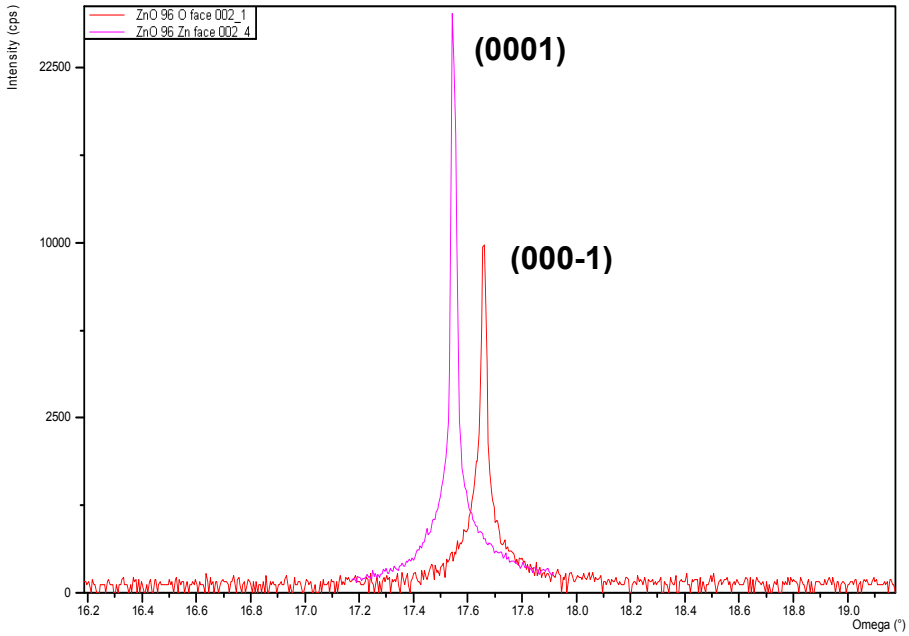

Fig. 2. X-ray diffraction rocking curves of {0001} surfaces of a high quality hydrothermal In:ZnO, full width at half maximum (FWHM) for the O face and Zn face are 0.1° and 0.05°.

3.2 Micro-Raman measurements

The Raman-active modes in ZnO crystals are $A_1+E_1+2E_2$. The A_1 and E_1 modes are polar and thus split into transverse (TO) and longitudinal (LO) components [17]. Unpolarized and polarized Raman spectra were measured on (0001), (000-1) natural faces and (11-20) cross-section of In:ZnO single crystals in the following backscattering geometries: $z(xy)\bar{z}$, $z(--)\bar{z}$ (unpolarized), $\bar{z}(xy)z$, $\bar{z}(--)z$ (unpolarized), and $x(--)\bar{x}$ (unpolarized) as shown in Fig.4. The frequencies observed in the spectra of In:ZnO, listed in Table 2, were compared with those found in our unintentionally-doped high quality ZnO, which was reported previously [18].

From the spectra measured on the cross-section, we found that the $E_2^2(high)$ peaks are shifted in the overgrown material within 100-150 μm off the growth interface, however, the strain is gradually relaxed as one moves away from the interface. The spectra measured on the c planes of In-doped ZnO sample contain nearly all the same peaks seen in unintentionally-doped ZnO. In addition, a weak peak exhibiting A_1 symmetry observed at 723 cm^{-1} is not seen in the undoped crystal. Broad spectral features in the range of 500-600 cm^{-1} found in hydrothermal bulk crystals doped with other impurities, e.g. Mn [17] are not seen in the bulk In-doped crystal. Similarly, several other peaks which were found in epitaxial ZnO films doped with a number of different metals such as Sb, Ga, and Al [7, 19] are not seen in our crystals. More interestingly, a peak at 312 cm^{-1} reported in hydrothermal In:ZnO

nanostructures [20] is not seen in our In-doped bulk crystal. These features may be specific defect-related and only occur in specific growth processes. It was reported that 531, 631, and 720 cm^{-1} modes were attributed to Sb, Ga, and Fe dopants. Therefore, we suspect that the mode 723 cm^{-1} in our case could also be related to Fe since Fe impurities were also detected in the In-doped ZnO crystal. In addition, the Raman bands measured in our In:ZnO are broader than the corresponding ones in undoped ZnO. These differences indicate that indium doping introduces lattice distortion, which is also consistent with the X-ray diffraction results shown in section 3.1.

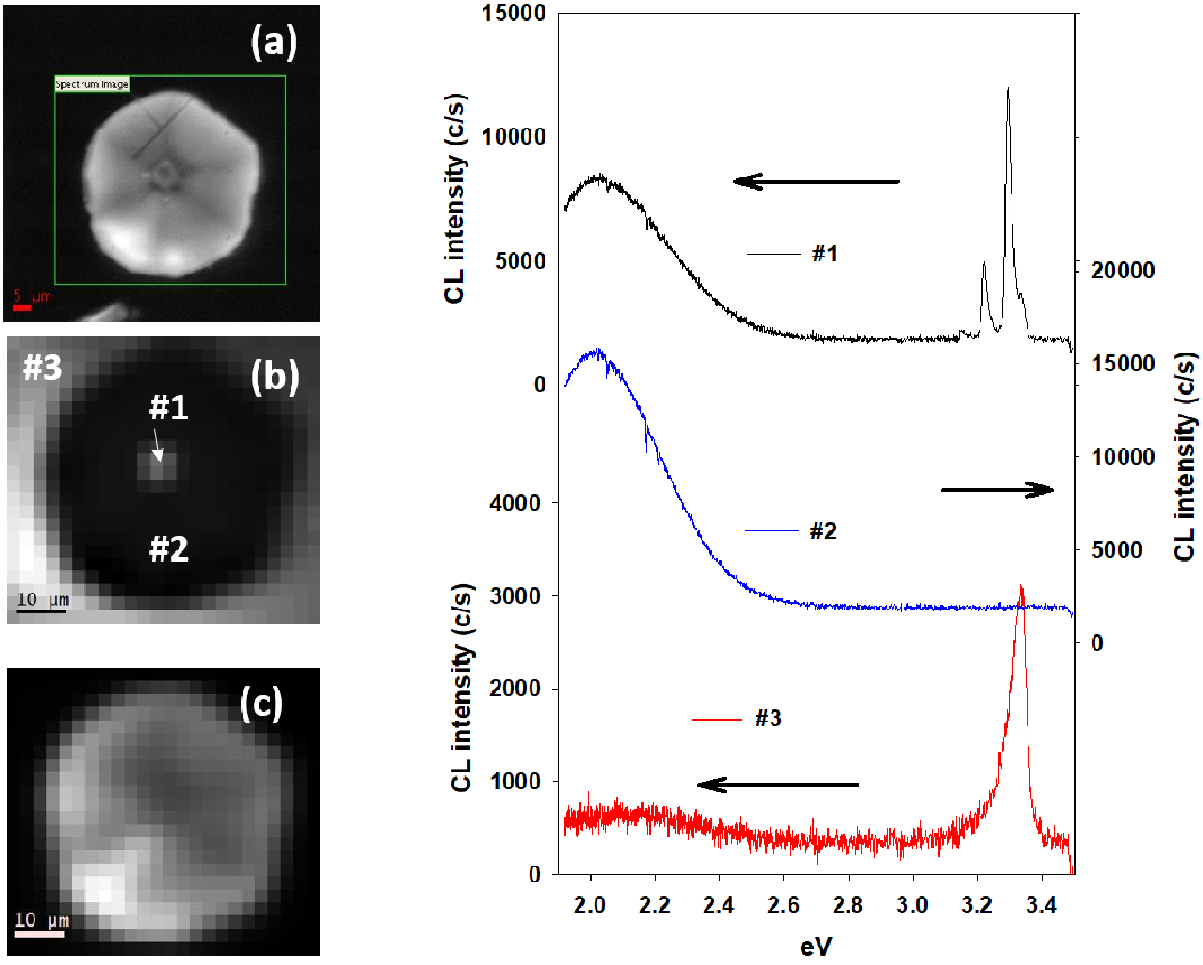

Fig. 3. (a) Panchromatic CL image of a hillock, (b) NBE monochromatic image of the hillock, (c) monochromatic (orange luminescence) CL image of the hillock, and (d) local CL spectra acquired in the points indicated in (b).

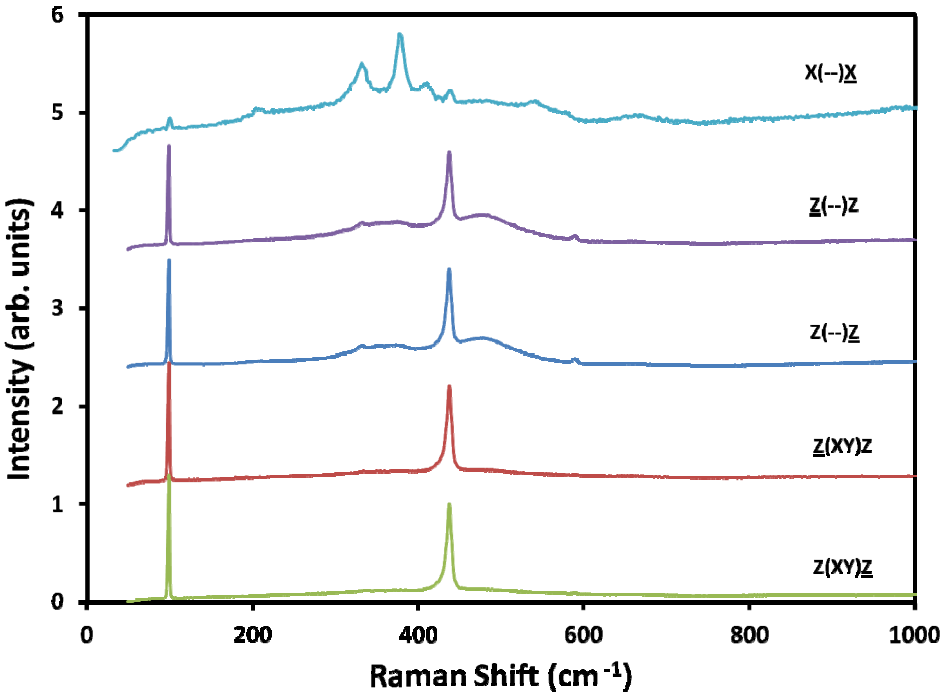

Fig. 4. Raman spectra measured on (0001) of a hydrothermal In:ZnO crystal in different backscattering geometries.

Table 2. Frequencies and symmetries of Raman peaks in hydrothermal In:ZnO in comparison with those in hydrothermal unintentionally-doped ZnO reported in [18]

In-doped ZnO (cm^{-1})	ZnO peaks (cm^{-1})	Symmetry of lines in In^{3+}:ZnO	Assignment in ZnO [18]
99	99	E_2^1 *(LO)*	
202	203	A_1	*2TA;* $2E_2^1$
289	284	A_1	$B_1^2 - B_1^1$
333	333	A_1	$E_2^2 - E_2^1$
377	378	$A_1\ (TO)$	
411	410	$E_1(TO)$	
438	438	$E_2^2(high)$	
479	483	A_1	*2LA*
540	536	A_1	$2B_1^1$
578	574	A_1	$A_1(LO)$
589		$E_1(LO)$	
660	657	A_1	*TA+LO*
723		A_1	
972	980	A_1+E_1+E_2	*2TO*
	1044	A_1+E_1+E_2	*TO+LO*
1104	1105	A_1+E_1+E_2	*2LO*
1151	1158	A_1+E_1+E_2	*2LO*

3.3 Photoluminescence measurements

The luminescence from bulk ZnO extends from the band edge to the green/orange spectral range with a common broad band centered around 2.45 eV. The sharp lines dominating the band edge region of the spectra originate from various bound exciton recombinations (excitons bound to neutral donors, D^0X, and/or acceptors, A^0X) followed by longitudinal optical (LO) phonon replicas with an energy separation of 72 meV [4]. At lower energies from 3.34 to 3.31 eV, two-electron satellite (TES) recombination lines of the neutral donor bound excitons are observed. In some samples a donor-acceptor-pair (DAP) transition at ~ 3.22 eV that is again followed by phonon replicas is found even though the chemical identity of the acceptor is unknown. On the high energy side of the bound excitons, free exciton transitions appear with the A-valence band (FXA) positioned at 3.377 eV.

We have performed photoluminescence (PL) measurements on a hydrothermal In:ZnO crystal. Fig. 5 shows the PL spectra measured at 2 K and demonstrates only a single strong narrow peak at 3.3586 eV with a few small peaks at 3.372-3.376 eV on the zinc face, and only one peak at 3.3577 eV on the oxygen face. We believe that the 3.3586 and 3.3577 eV are indium-related neutral donor bound exciton (In^0X) peaks since indium is the only dominant impurity in the crystals. The impurity analysis by secondary ion mass spectroscopy shows that the In:ZnO contains 1.38×10^{19} atoms/cm^{-3} of indium [9-10]. Photoluminescence spectra taken from the two faces reflects the varying emission peaks, impurity concentration, and defects at the surface. We believe the peak at 3.3586 eV is truly the indium peak, while peak at 3.3739 eV is the AT peak according to Meyer *et al*. Because in our crystals indium concentration is 60 times higher than lithium, and 17 times higher than sodium, the indium peak should be the dominant peak.

The peaks found in the hydrothermal ZnO doped with indium were slightly different from the ones reported in the literature [8] where I_9=3.3567 eV was assigned as the indium peak. The PL for bound exciton peaks were usually obtained from unintentionally doped ZnO crystals or films grown by other techniques. Our measurements deviation from published literature, as shown in Table 3, may result from growth strains and defects generated by indium dopants. It is known that bound excitons are extrinsic transitions and are related to dopants, native defects, or complexes, which usually create discrete electronic states in the bandgap, and therefore influence both optical absorption and emission processes. The recombination of bound excitons typically gives rise to sharp lines with a photon energy characteristic of each defect. Since the two faces may have doping concentrations and the indium-related donor bound exciton on two faces may be slightly different. Similarly, due to strains induced by doping, we had found that the gallium and aluminum-related neutral donor bound exciton (Ga^0X and Al^0X) peaks are the dominant peaks in Ga-doped and Al-doped ZnO crystals grown by a similar technique, and also deviated from the literature values (I_8 and I_6) [11]. It is worthwhile to note that all the donor bound excition ((D^0X) peaks reported in the literature were obtained from ZnO crystals/films without intentional doping and grown by other techniques.

Table 3. Comparison of excitation peaks of In, Ga and Al in PL of group III doped hydrothermal ZnO crystals with literature

	I_9 (In)	I_8 (Ga)	I_6 (Al)
Hydrothermal	3.3577	3.3604	3.3774
Literature [8]	3.3567	3.3598	3.3608

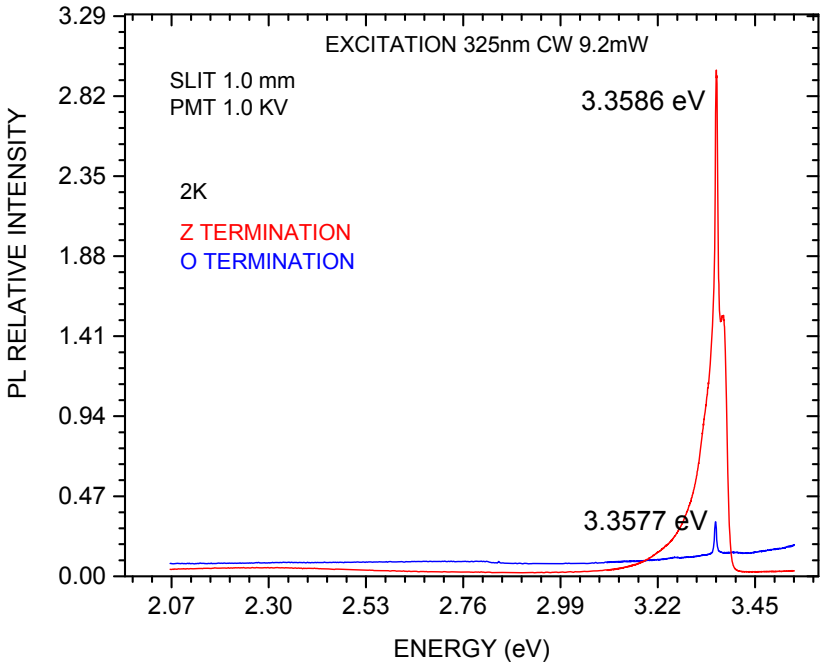

Fig.5. Photoluminescence spectra of an indium doped hydrothermal ZnO crystal using In_2O_3 as dopant

4 SUMMARY

Structural and optical properties of indium-doped highly-conductive ZnO bulk crystals grown by the hydrothermal technique have been studied. High resolution X-ray diffraction shows that the In-doped ZnO overgrew the Li-doped ZnO seed crystal pseudomorphically with some strains accumulated in the crystal, as supported by the expanded constant parameter *c* of the grown In:ZnO about 0.06% larger than from the Li-doped ZnO seed. Despite of growth hillocks on the {0001} faces, the overall quality of the grown crystals is of high quality. Photoluminescence spectra on both faces of In:ZnO show that indium donor bound exciton peak I_9 (In^0X) is the only dominated peak in the entire spectra, located at 3.3586eV on the zinc face and 3.3577 eV on the oxygen face, both of which deviated from literature value 3.3567 eV due to the strain in the crystal induced by indium doping. Raman scattering spectra of In:ZnO were measured in different backscattering geometries. The results show that strain at the regrowth interface relaxes within 100-150 μm, and the spectra measured on the c planes of In doped ZnO sample contain nearly all the same peaks seen in unintentionally-doped ZnO, indicating the crystal quality improves with the crystal grows. A weak peak is observed at 723 cm^{-1} which is not seen in the undoped crystal, while broad spectral features of in the range of 500-600 cm^{-1} found in hydrothermal Mn:ZnO crystals and the mode at 312 cm^{-1} observed in hydrothermal In:ZnO nanostructures do not appear in our In:ZnO bulk crystal, indicating that these features may be specific to certain defects in these materials.

ACKNOWLEDGEMENTS

We would like to thank Dr. Arnold Kiefer, Air Force Research Laboratory, Dayton, OH for help in X-ray diffraction.

REFERENCES

[1] C. Klingshirn, ZnO: From basics towards applications, Phys. Stat. Sol. (b) 244 (2007) 3027.

[2] D. C. Look, Progress in ZnO materials and devices, J. Electronic Materials, 35 (2006) 1299.

[3] T. Yanagida, Y. Fujimoto, A. Yoshikawa, Y. Yokota, et al., Scintillation properties of In doped ZnO with different In concentrations, IEEE Trans. on Nucl. Sci. 57 (2010) 1325.

[4] Ü. Özgür, Y. I. Alivov, C. Liu, A. Teke, M.A. Reshchikov, S. Dogan, V. Avrutin, S.-J. Cho and H. Morkoç, A comprehensive review of ZnO materials and devices, J. Appl. Phys. 98 (2005) 041301.

[5] D. Ehrentraut, H. Sato, M. Miyamoto, T. Fukuda, M. Nikl, K. Maeda, and I. Niikura, Fabrication of homoepitaxial ZnO films by low-temperature liquid-phase epitaxy, J. Cryst. Growth, 287 (2006) 367-371.

[6] M. D. McCluskey, S. J. Jokela, Defects in ZnO, J. Appl. Phys. 106 (2009) 071101.

[7] C. Bundemann, N. Ashkenov, M. Schubert, D. Spemann, T. Butz, E.M. Kaidashev, M. Lorenz, and M. Grundmann, Raman scattering in ZnO thin films doped with Fe, Sb, Al, Ga and Li, Appl. Phys. Lett. 83 (2003) 1974.

[8] B. K. Meyer, Chapter 7, Bound Exciton Complexes, in "Zinc Oxide: From Fundamental properties towards novel applications", eds C.F. Klingshirn, B.K. Meyer, A. Waag, A. Hoffmann and J. Geurts, Springer, 2010.

[9] Buguo Wang, M. Callahan, Chunchuan Xu, L.O. Bouthillette, N.C. Gile, D.F. Bliss, Hydrothermal growth and characterization of indium-doped-conducting ZnO crystals, J. Cryst. Growth, 304 (2007) 73–79.

[10] Buguo Wang, M. J. Callahan, L.O. Bouthillette, D.F. Bliss, and D. Look, Electrical, optical, and analytical characterization of bulk hydrothermal ZnO crystals doped with indium, J. Cryst. Growth, 319 (2011) 1-3.

[11] Buguo Wang, M. Mann, M. Snure, M. J. Callahan and D. Look, Hydrothermal Growth and Characterization of Ga-doped and Ga/N-codoped ZnO Crystals, SPIE proceedings, 8263, 826305 (2012).

[12] J. Jiménez and J. Tomm, Spectroscopic analysis of Optoelectronic Semiconductors (Springer, 2016, ISBN 978-3-319-42347-0).

[13] ZnO crystal structure data, JCPDS Card No. 36-1451.

[14] *CRC Handbook of Chemistry and Physics*, page D-183, 58th edition, 1978, CRC Handbook Press.

[15] Z. Galazka, R. Uecker, K. Irmscher, D. Schulz, D. Klimm, M. Albrecht, M. Pietsch, S. Ganschow, A. Kwasniewski, and R. Fornari, Melt growth, characterization and properties of bulk In_2O_3 single crystals, J. Cryst. Growth, 362 (2013) 349-352.

[16] D. F. Croxall, R. C. Ward, C. A. Wallace, and R. C. Kell, Hydrothermal Growth and Investigation of Li-Doped Zinc Oxide Crystals of High Purity and Perfection, J. Cryst. Growth 22 (1974) 117-124.

[17] L.N. Demyanets, R.M. Zakalyukin, and B.N. Marrin, Growth and Raman spectra of doped ZnO single crystals, Inorganic Mater. 47, 727-731, 2011.

[18] R. Cusco, E. Alarcon-Llado, H. Ibanez, L. Artus, J. Jimenez, Buguo Wang, M. J. Callahan, Temperature dependence of Raman scattering in ZnO, Phy. Rev. B 75, 165202 (2007).

[19] M.S. Jang, M.K. Ryu, M.H. Yoon, S.H. Lee, H.K. Kim, A. Onodera, S. Kojima, A study on the Raman spectra of Al-doped and Ga-doped ZnO ceramics, Current Applied Physics 9 (2009) 651–657.

[20] Escobedo-Morales A. and Pal U. "Effect of In, Sb and Ga doping on the structure and vibrational modes of hydrothermally grown ZnO nanostructures" Current Appl. Phys. 11 (2011) 525-531.

[21] T. Nakagawa, et al., Analysis of Indium Diffusion Profiles Based on the Fermi-Level Effect in Single-Crystal Zinc Oxide, Jpn. J. Appl. Phys. 46 (2007) 4099; 47 (2008) 7848.

[22] J. Kobayashi, et al., Properties of gallium- and aluminum-doped bulk ZnO obtained from single-crystals grown by liquid phase epitaxy, J. Cryst. Growth 311 (2009) 4408.

[23] Buguo Wang, M. Mann, Bruce Claflin, Michael Snure, David C. Look, Hydrothermal growth and characterization of aluminum-doped ZnO bulk crystals, Proc. of SPIE Vol. 8626, 862609 (2013).